European Journal of Nuclear Medicine and Molecular Imaging (2019) 46:2322–2328
https://doi.org/10.1007/s00259-019-04440-2

ORIGINAL ARTICLE

No differences in rest myocardial blood flow in stunned and hibernating myocardium: insights into the pathophysiology of ischemic cardiomyopathy

Dominik C. Benz[1] · Anita P. von Dahlen[1] · Wenjie Huang[1] · Michael Messerli[1] · Elia von Felten[1] · Georgios Benetos[1] · Andreas A. Giannopoulos[1] · Tobias A. Fuchs[1] · Christoph Gräni[1] · Catherine Gebhard[1] · Aju P. Pazhenkottil[1] · Oliver Gaemperli[1] · Philipp A. Kaufmann[1] · Ronny R. Buechel[1]

Received: 8 April 2019 / Accepted: 11 July 2019 / Published online: 29 July 2019

Abstract

Purpose The human pathophysiology of stunned, hibernating and scarred myocardium in ischemic cardiomyopathy is a subject of controversy. While the "smart heart" theory postulates that reduced myocardial blood flow (MBF) at rest is responsible for myocytes switching to a state of hibernation, other theories suggest that a reduced myocardial flow reserve (MFR) may be the cause.

Methods We included 110 patients with ischemic cardiomyopathy. Based on quantitative myocardial perfusion assessment and viability imaging with ^{13}N-NH3 and ^{18}F-FDG positron emission tomography, respectively, as well as wall motion assessment from echocardiography, myocardial tissue was characterized as remote (i.e., normal myocardium), stunned (i.e., dysfunctional but viable myocardium with normal rest perfusion), hibernating (i.e., dysfunctional but viable myocardium with impaired rest perfusion), or scarred myocardium (i.e., non-viable myocardium).

Results Compared to remote myocardium, dysfunctional but viable myocardium (including stunned and hibernating) had reduced rest MBF (0.89 mL/min/g vs. 0.79 and 0.76 mL/min/g, respectively; $p < 0.001$) and MFR (1.53 vs. 1.27 and 1.17; $p < 0.001$). Between stunned and hibernating myocardium, however, rest MBF and MFR did not differ ($p = 0.40$). In scarred myocardium, rest MBF was lowest (0.66 mL/min/g; $p < 0.001$) but, in contrast to the other myocardial states, k2 (i.e., tracer washout) was increased (0.199/min vs. 0.178/min to 0.181/min; all $p < 0.05$ in pairwise comparison).

Conclusions In patients with ischemic cardiomyopathy, impaired MFR is associated with stunning and hibernation. These states of dysfunctional but viable myocardium have lower rest MBF compared to remote myocardium. At the end of the continuum, rest MBF is lowest in scar tissue and linked to increased rate of tracer washout.

Keywords Stunning · Hibernating myocardium · Myocardial blood flow · Myocardial flow reserve · Viability testing

Introduction

Left ventricular (LV) dysfunction due to ischemic heart disease is associated with high morbidity and mortality and, in clinical routine, is successfully targeted by a variety of pharmacological and invasive treatment options [1]. The underlying pathophysiological mechanisms of LV dysfunction, however, are complex and a subject of controversy. The dysfunctional myocardial states have been identified as myocardial stunning, hibernation and scar [2]. In contrast to scar, most importantly, LV dysfunction can be reversed by revascularization in both myocardial stunning and hibernation. These two viable but chronically dysfunctional states differ with regard to myocardial perfusion at rest. While stunning is considered a state of prolonged LV dysfunction induced by an episode of ischemia with normal perfusion at rest [3], hibernation is associated with impaired perfusion at rest [4]. In his landmark editorial, Dr. Rahimtoola suggests that LV dysfunction is the smart reaction by which the heart copes with

Dominik C. Benz and Anita P. von Dahlen share first authorship

This article is part of the Topical Collection on Cardiology

✉ Ronny R. Buechel
ronny.buechel@usz.ch

[1] Department of Nuclear Medicine, Cardiac Imaging, University Hospital Zurich, Ramistrasse 100, CH-8091 Zurich, Switzerland

reduced rest myocardial blood flow (MBF) ("smart heart theory"). This notion, however, has been challenged by Camici and colleagues [5]. Based on animal and human studies [6, 7], the authors consider hibernation to be the result of repetitive stunning due to reduced myocardial flow reserve (MFR). Rest MBF was considered to be preserved. The aim of the present study was to characterize the different myocardial states by rest MBF, MFR, and washout as derived from ^{13}N-ammonia positron emission tomography (NH3-PET) in patients with ischemic cardiomyopathy.

Methods

Study population

We identified 110 patients with ischemic cardiomyopathy [i.e., left ventricular ejection fraction (LVEF) <55% and known coronary artery disease (CAD)] from the retrospective Zurich Quantitative PET Registry [8] who underwent combined NH3- and ^{18}F-fluorodeoxyglucose (FDG) PET to test for myocardial perfusion abnormalities and presence of hibernating myocardium at our institution between 2005 and 2015 and had wall motion assessment obtained from rest transthoracic echocardiography (TTE) within 3 months of PET if no cardiac event (i.e. CABG, PCI, myocardial infarction) had occurred between PET and TTE acquisition. Diabetic patients with poor myocardial FDG uptake were excluded ($n = 10$).

Positron emission tomography

Patients underwent NH3-PET at rest and during adenosine stress at a standard rate (0.14 mg/min/kg) over 7 min with 700–900 megabecquerels (MBq) of NH3 administered intravenously into a peripheral vein after 3 min into stress. For viability imaging, the injection of FDG was performed after a standardized oral glucose load [9]. After injection of 250 MBq of FDG, patients rested for about 1 h before image acquisition. Images were acquired either on a Discovery (LS/RX) PET/CT scanner or on an Advance PET scanner (both GE Healthcare, Waukesha, WI, USA), as previously reported in detail [10, 11]. Data were reconstructed as static, dynamic and gated images for NH3 perfusion imaging and as static images for FDG viability imaging.

For static images, polar maps were derived and displayed using the standardized 17-segment model. Segments were classified as ischemic, stunned, hibernating, and scarred as previously described [12]. In short, scoring was based on relative tracer uptake with a score of 0 (normal) to 4 (absent) [13]. All segments that were unaffected by perfusion abnormalities in static imaging were defined as "normally perfused", remote myocardium. Ischemia, hibernating myocardium and scar were scored as previously published. Ischemia was determined per segment from the difference between the summed stress and rest scores. Hibernating myocardium was scored per segment from the positive difference between the summed rest score and the FDG score (resulting in the hibernation score). Scar was computed per segment from the positive difference between the summed rest score and the hibernation score. Segments that were scored mixed with ischemia, hibernation and/or scar were excluded from the analysis to guarantee unbiased results.

In dynamic images, a volume of interest (VOI) encompassing the LV myocardium was drawn, and two additional VOIs were placed into the blood pool of the left and right ventricle. Myocardial and blood pool time–activity curves (TAC) were obtained from dynamic frames corrected for radioisotope decay. A two-compartment model corrected for spillover and partial volume effects was used to calculate MBF and k2 (i.e., the NH3 washout constant rate) using a commercially available software (PMOD, version 3.7; PMOD Technologies Ltd., Zurich, Switzerland) developed and validated at our institution [14]. The volume of distribution (VD; mL/g) of the extravascular compartment was used as a parameter of metabolic retention of NH3 and was calculated as rest MBF over k2. The metabolic retention of NH3 (in the form of glutamine) reduces k2 and, as a result, increases the VD of the extravascular compartment implying intact NH3 metabolism [15]. Myocardial flow reserve (MFR) was calculated as the ratio of hyperemic MBF over rest MBF. The following tracer-specific conversion factors were applied to calculate effective radiation dose from the administered activity: 0.0019 mSv/MBq for FDG and 0.002 mSv/MBq for NH3 [16].

Evaluation of EF and wall motion abnormality

Post-stress and rest LVEF from PET were computed from gated stress or rest perfusion images, respectively. From TTE, LVEF and abnormal wall motion were assessed semiquantitatively and visually, respectively, and defined per segment as hypokinetic, dyskinetic or akinetic wall motion.

Definition of myocardial states

Based on the relative distribution of NH3 and FDG myocardial uptake and on wall motion assessment obtained from TTE, myocardium was classified on a segment level. In brief, remote myocardium was defined as normal stress perfusion and wall motion, stunned myocardium as ischemia with abnormal wall motion, hibernating myocardium as viable tissue with abnormal rest perfusion and wall motion, and scar as non-viable tissue with abnormal wall motion.

Statistical analysis

Continuous variables were expressed as median with interquartile range (IQR), as all data were not normally distributed, and categorical variables as percentages. The Kolmogorov–Smirnov test was applied to assess normal distribution. Comparison of continuous variables with non-normal distributions between groups was performed with Mann–Whitney *U* test and Kruskal–Wallis test. A p value <0.05 was considered statistically significant. SPSS version 20.0 software (IBM Corporation, Armonk, NY, USA) was used for analysis.

Results

Study population

The baseline characteristics of the study population ($n = 110$) are summarized in Table 1. The imaging findings are listed in Table 2. Of note, in the 22 patients with recent myocardial infarction (within 3 months), the extent of hibernating myocardium was significantly larger (8.8% vs. 4.3% of LV myocardium; $p = 0.013$). All other imaging findings (i.e. hyperemic MBF, rest MBF, MFR, k2, VD, ischemia extent and scar extent), however, did not differ significantly (all $p > 0.05$). Mean effective radiation exposure was 8.8 ± 1.6 mSv (3.9 ± 1.5 mSv from NH3-PET and 4.9 ± 0.6 mSv from FDG-PET).

Myocardial states

Of 1870 segments in 110 patients, 904 segments (48%) could be classified into a myocardial state according to the predefined features. The other segments were either excluded because they were classified as mixed (280 segments, 15%) or because they did not match the strict definition for the tissue characterization (686 segments, 37%), e.g. remote myocardium that was dysfunctional or scar tissue that was not dysfunctional. The proportion of segments excluded did not differ between patients with and without diabetes (52% vs. 51%; $p = 0.531$). From the resulting 904 analyzed myocardial segments, 312 segments (35%) were characterized as remote, 130 (14%) as stunned, 136 (15%) as hibernating, and 326 (36%) as scarred.

Quantitative parameters among different tissues

Hyperemic MBF, rest MBF, MFR and VD differed significantly ($p < 0.001$) and k2 trended towards a difference ($p = 0.054$) between the various myocardial tissues (Table 3). In detail, rest MBF did not differ between stunned and hibernating myocardium (0.79 mL/min/g vs. 0.76 mL/min/g; $p = 0.732$), but it was significantly lower than in remote myocardium (0.89 mL/min/g; $p < 0.001$) and significantly higher than in scarred myocardium (0.66 mL/min/g, $p < 0.001$). Furthermore, while MFR was lower in hibernating compared to stunned myocardium, the difference did not reach statistical significance (1.17 vs. 1.27; $p = 0.405$). Interestingly, VD and k2—two markers of metabolic cell integrity—had significantly lower values (3.56 mL/g vs. 4.49 to 5.31 mL/g; $p < 0.001$)

Table 1 Baseline patient characteristics ($n = 110$)

Characteristics	
Male gender, *n* (%)	95 (86)
Age (years)	68 [59–76]
Body mass index (kg/m^2)	26.3 [24.3–29.5]
Cardiac risk factors, *n* (%)	
Smoking	67 (61)
Diabetes mellitus	39 (36)
Hypertension	82 (75)
Dyslipidemia	74 (67)
Family history of CAD	34 (31)
Symptoms, *n* (%)	
Asymptomatic	15 (14)
Typical chest pain	30 (27)
Atypical chest pain	4 (4)
Unclear chest pain	9 (8)
Dyspnea	77 (70)
Medication, *n* (%)	
Beta blockers	88 (80)
ACEi/ARB	95 (86)
Diuretics	73 (66)
Antithrombotics	86 (78)
Anticoagulation	38 (35)
Statin	94 (86)
Cardiac history, *n* (%)	
Known CAD	108 (98)
1-vessel CAD	*16 (15)*
2-vessels CAD	*24 (22)*
3-vessels CAD	*68 (63)*
Myocardial infarction	79 (72)
Previous PCI	52 (47)
Previous CABG	40 (36)
EF (%)	33 [26–41]
Concomitant diseases, *n* (%)	
Atrial fibrillation	28 (26)
Mitral regurgitation	65 (59)
Renal failure (eGFR <60)	47 (43)

If not otherwise specified, values given are median and, in [brackets] interquartile range

CAD coronary artery disease, *ACEi* angiotensin-converting enzyme inhibitor, *ARB* angiotensin receptor blocker, *PCI* percutaneous coronary intervention, *CABG* coronary artery bypass graft, *EF* ejection fraction, *eGFR* estimated glomerular filtration rate

Table 2 Imaging findings

PET	
Post-stress EF (%)	26 [19–34]
Rest EF (%)	26 [19–34]
Hyperemic MBF (mL/min/g)	1.06 [0.89–1.28]
Rest MBF (mL/min/g)	0.78 [0.67–0.98]
MFR	1.28 [1.07–1.62]
k2 (/min)	0.194 [0.136–0.255]
VD (mL/g)	4.25 [3.02–6.08]
Ischemia, *n* (%)	89 of 108 (82)
Ischemia extent (%)	3.7 [1.5–5.9]
≤5%, *n* (%)	55 (62)
>5% to ≤ 10%, *n* (%)	22 (25)
>10% to ≤ 20%, *n* (%)	10 (11)
>20%, *n* (%)	2 (2)
Hibernating, *n* (%)	85 of 109 (78)
Hibernating extent (%)	2.9 [1.5–7.4]
≤5%, *n* (%)	46 (54)
>5% to ≤ 10%, *n* (%)	21 (25)
>10% to ≤ 20%, *n* (%)	15 (18)
>20%, *n* (%)	3 (4)
Scar, *n* (%)	101 of 109 (93)
Scar extent (%)	10.3 [5.9–16.9]
≤5%, *n* (%)	13 (13)
>5% to ≤ 10%, *n* (%)	29 (29)
>10% to ≤ 20%, *n* (%)	42 (42)
>20%, *n* (%)	17 (17)
Transthoracic echocardiography	
EF (%)	33 [26–41]
Any wall motion abnormality, *n* (%)	110 of 110 (100)

If not otherwise specified, values given are median and, in [brackets], interquartile range

EF ejection fraction, *MBF* myocardial blood flow, *MFR* myocardial flow reserve, *VD* volume of distribution

and trended towards higher values (0.199/min vs. 0.178 to 0.181/min; $p = 0.054$), respectively, in scarred myocardium (Fig. 1).

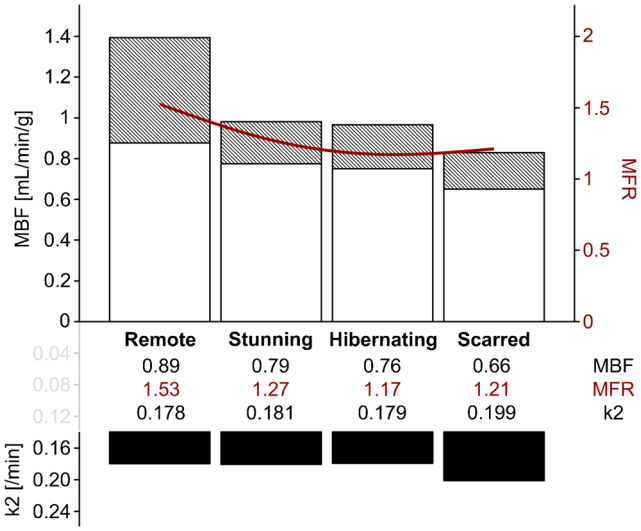

Fig. 1 The figure illustrates and summarizes the continuum of myocardial states from remote, "normally" perfused myocardium, to stunned and then to hibernating. At the end of the continuum is scar. White bars indicate rest MBF. At stress, MBF is enhanced by gray layers on top of white bars; combining white and gray layers visualizes stress MBF. MFR is indicated by gray layers and by the red line. Black bars indicate tracer washout (i.e. k2). Values given are median rest MBF, MFR and k2 for remote, stunned, hibernating and scarred myocardium, respectively

Discussion

The present study may offer valuable insights into the pathophysiology of different myocardial states in ischemic cardiomyopathy. In accordance with the "smart heart theory" [4], rest MBF was reduced in hibernating compared to remote myocardium. In fact, our MBF values correspond well to the weighted mean of previous studies in a similar population [2]. The present study, however, extends the comparison to stunned myocardium, which in the present study had rest MBF similar to hibernating myocardium. This is contrary to experimental studies in pigs [17], which gave rise to the hypothesis that stunned myocardium should exhibit normal rest MBF. In these studies, nonetheless, rest MBF decreased with disease progression and over time, and stunned myocardium transformed into hibernating myocardium. These findings laid

Table 3 Quantitative parameters among different myocardial states

	Remote ($n = 312$)	Stunned ($n = 130$)	Hibernating ($n = 136$)	Scar ($n = 326$)	*p* value
Hyperemic MBF	1.39$^{\circ+}$ [1.14–1.84]	0.98* [0.73–1.31]	0.97* [0.68–1.19]	0.83*$^{\circ}$ [0.58–1.17]	<0.001
Rest MBF	0.89$^{\circ+}$ [0.73–1.08]	0.79* [0.63–0.93]	0.76* [0.63–0.99]	0.66*$^{\circ+}$ [0.54–0.86]	<0.001
MFR	1.53$^{\circ+}$ [1.22–1.96]	1.27* [0.98–1.60]	1.17* [0.94–1.48]	1.21* [0.95–1.60]	<0.001
k2	0.178 [0.116–0.238]	0.181 [0.099–0.277]	0.179 [0.122–0.252]	0.199*$^{\circ+}$ [0.125–0.301]	0.054
VD	5.31 [3.71–8.00]	4.49 [3.07–7.78]	4.70 [3.14–6.78]	3.56*$^{\circ+}$ [2.30–6.07]	<0.001

Values given are median and, in [brackets], interquartile range. Post hoc Kruskal–Wallis pairwise comparisons with adjustment for multiple tests by Bonferroni correction revealed a significant difference compared to remote (*), stunned (°) and hibernating myocardium ($^{+}$)

MBF myocardial blood flow, *MFR* myocardial flow reserve, *VD* volume of distribution

the conceptual framework linking repetitive ischemia, chronic stunning and hibernation as a continuum. In the present study, the reduced rest MBF in stunned myocardium may thus be due to a more advanced stage of the disease. If the delay in the recovery of stunning outlasts the interval between ischemic episodes—as in the chronically stunned myocardium in the present study—the tissue may undergo substantial functional and structural adaptations. Therefore, the present findings do not necessarily disagree with, but rather complement and potentially complete, the continuum. Additionally, the findings of experimental animal studies do not directly translate to a heterogeneous human population in a real-world setting. It seems important to bear in mind that the present findings are a quantitative description of the different myocardial states at an advanced stage of the disease, with multiple myocardial infarctions and revascularizations, influenced by collateral flow and interspersed with fibrosis, rather than an experimental study to validate the concept of human pathophysiology.

Furthermore, the lower rest MBF in dysfunctional but viable myocardium deserves closer attention. Indeed, the heart seems to be smart: when blood supply is running short, myocardial contraction is restricted as part of an act of self-preservation [4]. However, as outlined by Camici and colleagues [5], the unifying characteristic emerging from most animal and human studies is an impaired MFR in chronically dysfunctional myocardium. Our findings corroborate this concept: stunning, like hibernation, is characterized by a reduced MFR as compared to remote myocardium (1.27 and 1.17 vs. 1.53). Although the difference in MFR between stunning and hibernation did not reach statistical significance, the decreasing MFR supports the notion that myocardial states are a continuum ranging from stunning to hibernation, with deterioration into the latter once MFR falls below a critical threshold. Under these circumstances, any increase in cardiac workload, even ordinary daily activities, leads to myocardial ischemia (followed by post-ischemic stunning), eventually resulting in chronic dysfunction [18]. A restriction in contractility may preserve energy and, thus, may exhibit as lower rest MBF. In the present study, the reduction of rest MBF by 11% from remote myocardium with normal LV function to chronically dysfunctional myocardium seems coherent with this reasoning, and corresponds well to other human studies [19]. As a result, the downregulation of rest MBF has been considered as the effect of the dysfunctional myocardium's reduced energy demand, rather than the cause for LV dysfunction [2].

Although the concept is fundamental for our understanding of human myocardial pathophysiology, its relevance from a clinical perspective is vague. In the management of the patient, the primary concern is whether dysfunctional myocardium with impaired rest perfusion is reversible by revascularization, regardless of whether it is stunned or hibernating. Most importantly, if such myocardium has reached the end of the continuum, that is, scar, revascularization can be deferred safely. The lack of difference in MFR between hibernating myocardium and scar indicates that other factors (e.g. severity and course of myocardial ischemia) might influence the natural history of the myocardial cells. In the present study, scar had the lowest MBF. Moreover, tracer washout as a marker of metabolic integrity was unchanged in remote, stunned or hibernation, but increased in scar tissue. Again, the values found in the present study compare well with the existing literature [15]. Consequently, since scar tissues delineate so clearly from viable myocardium, rest MBF and tracer washout were proposed as useful tools for predicting viability and reversibility of LV dysfunction. Indeed, two pilot studies revealed promising results [15, 20]. A more recent, larger study, however, found only a low diagnostic performance of NH3 tracer kinetics in predicting viable myocardium [21]. Nevertheless, the added clinical value of quantification of MBF and calculation of MFR by PET has been demonstrated in a multitude of settings (e.g. coronary artery disease, diabetes, kidney disease, non-ischemic cardiomyopathy) and might impact patient management [22–27].

We acknowledge the following limitations. The present data have been collected retrospectively in a clinical setting. Hence, the included patient population is heterogeneous, at different stages of the disease and with comorbidities. In addition, due to the retrospective design, information on reversibility after revascularization has not been available. Future studies should investigate the predictive value of rest MBF, MFR and tracer washout on the reversibility of LV dysfunction. Furthermore, including only 48% of all segments in the present analysis limits the generalizability of the present study. Nonetheless, the exclusion of segments that were classified as mixed or did not match the strict definition for tissue characterization guaranteed unbiased results.

Conclusions

In patients with ischemic cardiomyopathy, impaired MFR is associated with stunning and hibernation. These states of dysfunctional but viable myocardium have lower rest MBF compared to remote myocardium. At the end of the continuum, rest MBF is lowest in scar tissue and linked to increased rate of tracer washout.

Acknowledgements We thank Verena Weichselbaumer, Martina Vogt, Tania Lagrange, Kevin Frei, Kathrin Amsler, Frederic Koszarski und Bejtulah Salahi for their excellent technical support.

Compliance with ethical standards

Conflict of interest The University Hospital Zurich holds a research agreement with GE Healthcare. Dominik C. Benz has received research grants from the Theodor and Ida Herzog-Egli Foundation. Anita Schneider declares that she has no conflict of interest. Wenjie Huang

declares that he has no conflict of interest. Michael Messerli declares that he has no conflict of interest. Elia von Felten declares that he has no conflict of interest. Georgios Benetos declares that he has no conflict of interest. Andreas A. Giannopoulos declares that he has no conflict of interest. Tobias A. Fuchs declares that he has no conflict of interest. Christoph Gräni declares that he has no conflict of interest. Catherine Gebhard declares that he has no conflict of interest. Aju P. Pazhenkottil declares that he has no conflict of interest. Oliver Gaemperli declares that he has no conflict of interest. Philipp A. Kaufmann declares that he has no conflict of interest. Ronny R. Buechel declares that he has no conflict of interest.

Ethical approval All procedures performed in studies involving human participants were in accordance with the ethical standards of the local research committee (Ethics Committee Zurich, BASEC-Nr. 2016-00177) and with the 1964 Helsinki declaration and its later amendments or comparable ethical standards.

Informed consent Informed consent was waived for all patients scanned before 2014 due to subsequent use of non-genetic personal health data only. For all patients scanned afterward (after the adoption of a new law in Switzerland), written informed consent was obtained.

References

1. Ponikowski P, Voors AA, Anker SD, Bueno H, Cleland JG, Coats AJ, et al. 2016 ESC guidelines for the diagnosis and treatment of acute and chronic heart failure: the task force for the diagnosis and treatment of acute and chronic heart failure of the European Society of Cardiology (ESC) developed with the special contribution of the heart failure association (HFA) of the ESC. Eur Heart J. 2016;37:2129–200. https://doi.org/10.1093/eurheartj/ehw128.
2. Canty JM, Fallavollita JA. Chronic hibernation and chronic stunning: a continuum. J Nucl Cardiol. 2000;7:509–27. https://doi.org/10.1067/mnc.2000.109683.
3. Benz DC, Gaemperli O. The right timing for post-ischemic stunning. J Nucl Cardiol. 2017;24:1302–4.
4. Rahimtoola SH. The hibernating myocardium. Am Heart J. 1989;117:211–21.
5. Camici PG, Wijns W, Borgers M, De Silva R, Ferrari R, Knuuti J, et al. Pathophysiological mechanisms of chronic reversible left ventricular dysfunction due to coronary artery disease (hibernating myocardium). Circulation. 1997;96:3205–14.
6. Vanoverschelde JL, Wijns W, Depre C, Essamri B, Heyndrickx GR, Borgers M, et al. Mechanisms of chronic regional postischemic dysfunction in humans. New insights from the study of noninfarcted collateral-dependent myocardium. Circulation. 1993;87:1513–23.
7. Gerber BL, Vanoverschelde JL, Bol A, Michel C, Labar D, Wijns W, et al. Myocardial blood flow, glucose uptake, and recruitment of inotropic reserve in chronic left ventricular ischemic dysfunction. Implications for the pathophysiology of chronic myocardial hibernation. Circulation. 1996;94:651–9.
8. Benz DC, Gräni C, Ferro P, Neumeier L, Messerli M, Possner M, et al. Corrected coronary opacification decrease from coronary computed tomography angiography: validation with quantitative 13N-ammonia positron emission tomography. J Nucl Cardiol. 2017. https://doi.org/10.1007/s12350-017-0980-2.
9. Tillisch J, Brunken R, Marshall R, Schwaiger M, Mandelkern M, Phelps M, et al. Reversibility of cardiac wall-motion abnormalities predicted by positron tomography. N Engl J Med. 1986;314:884–8. https://doi.org/10.1056/NEJM198604033141405.
10. Herzog BA, Husmann L, Valenta I, Gaemperli O, Siegrist PT, Tay FM, et al. Long-term prognostic value of 13N-ammonia myocardial perfusion positron emission tomography added value of coronary flow reserve. J Am Coll Cardiol. 2009;54:150–6. https://doi.org/10.1016/j.jacc.2009.02.069.
11. Steffen DA, Giannopoulos AA, Grossmann M, Messerli M, Schwyzer M, Gräni C, et al. "apical thinning": relations between myocardial wall thickness and apical left ventricular tracer uptake as assessed with positron emission tomography myocardial perfusion imaging. J Nucl Cardiol. 2018. https://doi.org/10.1007/s12350-018-1397-2.
12. Ling LF, Marwick TH, Flores DR, Jaber WA, Brunken RC, Cerqueira MD, et al. Identification of therapeutic benefit from revascularization in patients with left ventricular systolic dysfunction: inducible ischemia versus hibernating myocardium. Circ Cardiovasc Imaging. 2013;6:363–72. https://doi.org/10.1161/circimaging.112.000138.
13. Verberne HJ, Acampa W, Anagnostopoulos C, Ballinger J, Bengel F, De Bondt P, et al. EANM procedural guidelines for radionuclide myocardial perfusion imaging with SPECT and SPECT/CT: 2015 revision. Eur J Nucl Med Mol Imaging. 2015;42:1929–40. https://doi.org/10.1007/s00259-015-3139-x.
14. Siegrist PT, Gaemperli O, Koepfli P, Schepis T, Namdar M, Valenta I, et al. Repeatability of cold pressor test-induced flow increase assessed with H(2)(15)O and PET. J Nucl Med. 2006;47:1420–6.
15. Beanlands RS, deKemp R, Scheffel A, Nahmias C, Garnett ES, Coates G, et al. Can nitrogen-13 ammonia kinetic modeling define myocardial viability independent of fluorine-18 fluorodeoxyglucose? J Am Coll Cardiol. 1997;29:537–43.
16. Hesse B, Tägil K, Cuocolo A, Anagnostopoulos C, Bardiés M, Bax J, et al. EANM/ESC procedural guidelines for myocardial perfusion imaging in nuclear cardiology. Eur J Nucl Med Mol Imaging. 2005;32:855–97. https://doi.org/10.1007/s00259-005-1779-y.
17. Fallavollita JA, Canty JM. Differential 18F-2-deoxyglucose uptake in viable dysfunctional myocardium with normal resting perfusion: evidence for chronic stunning in pigs. Circulation. 1999;99:2798–805.
18. Braunwald E, Kloner RA. The stunned myocardium: prolonged, postischemic ventricular dysfunction. Circulation. 1982;66:1146–9.
19. Camici PG, Dutka DP. Repetitive stunning, hibernation, and heart failure: contribution of PET to establishing a link. Am J Physiol Heart Circ Physiol. 2001;280:H929–36. https://doi.org/10.1152/ajpheart.2001.280.3.H929.
20. Gewirtz H, Fischman AJ, Abraham S, Gilson M, Strauss HW, Alpert NM. Positron emission tomographic measurements of absolute regional myocardial blood flow permits identification of nonviable myocardium in patients with chronic myocardial infarction. J Am Coll Cardiol. 1994;23:851–9.
21. Benz DC, Ferro P, Safa N, Messerli M, von Felten E, Huang W, et al. Role of quantitative myocardial blood flow and ^{13}N-ammonia washout for viability assessment in ischemic cardiomyopathy. J Nucl Cardiol. 2019. https://doi.org/10.1007/s12350-019-01684-1.
22. Murthy VL, Naya M, Foster CR, Hainer J, Gaber M, Di Carli G, et al. Improved cardiac risk assessment with noninvasive measures of coronary flow reserve. Circulation. 2011;124:2215–24. https://doi.org/10.1161/circulationaha.111.050427.
23. Gebhard C, Fiechter M, Herzog BA, Lohmann C, Bengs S, Treyer V, et al. Sex differences in the long-term prognostic value of. Eur J Nucl Med Mol Imaging. 2018;45:1964–74. https://doi.org/10.1007/s00259-018-4046-8.

24. Murthy VL, Naya M, Foster CR, Gaber M, Hainer J, Klein J, et al. Association between coronary vascular dysfunction and cardiac mortality in patients with and without diabetes mellitus. Circulation. 2012;126:1858–68. https://doi.org/10.1161/circulationaha.112.120402.
25. Murthy VL, Naya M, Foster CR, Hainer J, Gaber M, Dorbala S, et al. Coronary vascular dysfunction and prognosis in patients with chronic kidney disease. JACC Cardiovasc Imaging. 2012;5:1025–34. https://doi.org/10.1016/j.jcmg.2012.06.007.
26. Neglia D, Michelassi C, Trivieri MG, Sambuceti G, Giorgetti A, Pratali L, et al. Prognostic role of myocardial blood flow impairment in idiopathic left ventricular dysfunction. Circulation. 2002;105:186–93.
27. Taqueti VR, Hachamovitch R, Murthy VL, Naya M, Foster CR, Hainer J, et al. Global coronary flow reserve is associated with adverse cardiovascular events independently of luminal angiographic severity and modifies the effect of early revascularization. Circulation. 2015;131:19–27. https://doi.org/10.1161/CIRCULATIONAHA.114.011939.